Real-time monitoring of cardiac radio-frequency ablation lesion formation using an optical coherence tomography forward-imaging catheter

Christine P. Fleming,[a] Hui Wang,[a] Kara J. Quan,[b,*] and Andrew M. Rollins[a,†]

[a]Case Western Reserve University, Biomedical Engineering Department, Cleveland, Ohio 44106
[b]MetroHealth Medical Center, Heart and Vascular Center, Cleveland, Ohio 44109

Abstract. Radio-frequency ablation (rfa) is the standard of care for the treatment of cardiac arrhythmias; however, there are no direct measures of the successful delivery of ablation lesions. Optical coherence tomography (OCT) imaging has the potential to provide real-time monitoring of cardiac rfa therapy, visualizing lesion formation and assessing tissue contact in the presence of blood. A rfa-compatible forward-imaging conical scanning probe is prototyped to meet this need. The forward-imaging probe provides circular scanning, with a 2-mm scan diameter and 30-μm spot size. During the application of rf energy, dynamics are recorded at 20 frames per second with a 40-kHz A-line rate. Real-time monitoring of cardiac rfa lesion formation and imaging in the presence of blood is demonstrated *ex vivo* in a swine left ventricle with a forward, flexible, circular scanning OCT catheter. [DOI: 10.1117/1.3459134]

Keywords: radio-frequency ablation; optical coherence tomography; cardiac imaging; catheter.

Paper 10122LR received Mar. 11, 2010; revised manuscript received May 28, 2010; accepted for publication Jun. 1, 2010; published online Jul. 1, 2010.

1 Introduction

Cardiac arrhythmias are a major source of morbidity and mortality in the United States.[1] Radio-frequency ablation (rfa) directed at interrupting critical components of arrhythmia circuits is the standard of care for the treatment of tachyarrhythmias. Current techniques for anatomical guidance of ablation therapy utilize low-resolution 2-D fluoroscopic images or static images from computed tomography merged onto fluoroscopy. Monitoring of rfa is by indirect means, such as assessment of tissue temperature, power delivery, and impedance at the tip of the ablation catheter. This indirect method of monitoring can often result in delivering more rfa lesions than necessary to achieve a therapeutic effect, prolonging procedure times and thereby increasing the risk of these procedures. Intracardiac echocardiography monitors rfa therapy in real time to assess catheter-tissue contact and contact angle,[2] visualize stenosis of pulmonary vessels[2] and embolic events. However, intracardiac echocardiography does not have sufficient contrast to visualize the formation of rfa lesions. Additional technology for directly monitoring ablation lesion formation during procedures in real time can further decrease procedural time and improve patient and operator safety.

Optical coherence tomography (OCT) is an emerging modality that provides high-resolution, depth-resolved imaging of tissue microstructures.[3] OCT has demonstrated the ability to distinguish ablated from untreated tissue,[4] and image the atrioventricular node,[5] and abnormal fiber organization[5,6] within *ex vivo* cardiac animal models. To translate OCT technology, optical catheters have been developed for imaging internal structures, and have been used for gastrointestinal endoscopy[7] and intravascular imaging.[8] A variety of designs have been employed including forward-imaging[9–11] and side-viewing catheter.[12] Designing a forward-imaging catheter that is both small in diameter and flexible presents many challenges. Others have designed probes with distal actuation to provide a wide range of scanning patterns.[9,13,14] However, these catheters are not easily miniaturized, as the scanning mechanism limits the outer diameter of the catheter tip. Proximal actuation has been shown,[10] but the probe was rigid.

In this work, we present real-time imaging of rfa lesion formation and imaging in the presence of blood with a flexible, forward-imaging OCT catheter.

2 Methods and Results

Cardiac rfa lesions are formed most effectively if the ablation catheter is perpendicular and has adequate contact with the tissue. Therefore, a flexible forward-scanning OCT catheter was designed and prototyped that allows for in-contact, circular-scan imaging (Fig. 1). Light is delivered via a SMF28e optical fiber, the beam is focused by a GRIN lens, deflected 1-mm off-axis by a Risley prism, and a fused-silica optical window isolates the probe interior from the tissue environment [Fig. 1(a)]. The mechanical support was designed from glass, ceramic, and polymer materials (no metal) to avoid thermal effects and interference in close proximity to the rfa catheter [Fig. 1(b)]. Rotary motion imparted by torque applied to the fiber proximally, at the fiber rotary joint, allowed for circular scanning. The rigid portion of the catheter was 18 mm in length and the outer diameter was 2.5 mm. Polytetrafluorethylene moisture seal heat shrink tubing was placed on the probe end cap, increasing the outer diameter at the probe tip to 3.2 mm. The spot diameter of the design is 28-μm full-width at half-maximum (FWHM), with minimal aberrations over 1 mm of axial scan range from the optical glass [Fig. 1(c)]. Spot profiles measured using a beam analyzer [Fig. 1(d)] were circular, clean, and under 30 μm.

The forward-imaging catheter was integrated into a Fourier domain OCT system.[15] A superluminescent diode centered at 1310 nm with a 75-nm (FWHM) bandwidth was used for the light source (Inphenix, Livermore, California). A linear in wave-number ($k=2\pi/\lambda$) spectrometer[15] was used to project spectral interference fringes onto a 1024-pixel InGaAs line-

*Currently with North Ohio Heart Center, Cardiac Electrophysiology, Elyria, OH 44035.
†Address all correspondence to: Andrew M. Rollins, E-Mail: rollins@cwru.edu

1083-3668/2010/15(3)/030516/3/$25.00 © 2010 SPIE

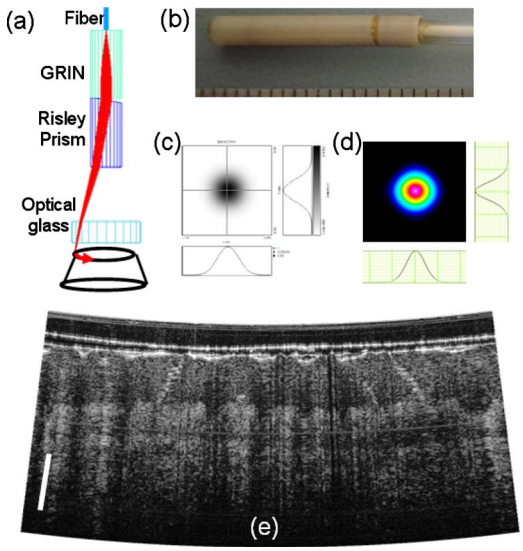

Fig. 1 OCT forward-imaging probe. (a) Schematic of probe for circular scanning, GRIN lens used for focusing, Risley prism to deflect beam off axis, optical glass to isolate probe from environment. Rotation of assembly produces circular scanning. (b) Close-up of proximal end of probe. (c) Spot profile from ASAP simulation and (d) measured from prototype catheter showing a 28-μm FWHM spot size. (e) *In vivo* human skin image at 10 fps. 500-μm scale bar.

scan camera (Goodrich, Princeton, New Jersey). The system had a 4.3-mm imaging range, 2-mm −6-dB fall off, 115-dB signal-to-noise ratio, and 11-μm axial resolution (in tissue). An image of *in vivo* human thick skin taken at 10 frames per second (fps) with 4000 lines per frame (lpf) is shown in Fig. 1(e).

Visualizing real-time ablative lesion formation using the forward-imaging catheter was demonstrated using ventricular wedges from a freshly excised swine heart. Following the onset of general anesthesia, a lateral thoracotomy was performed, and the heart was rapidly excised and placed in ice-cold phosphate buffered saline (PBS). Individual sections of left ventricular muscle were placed in a custom chamber with PBS maintained at 37 °C. The OCT forward-imaging probe was bound side by side to the rfa catheter [Fig. 2(a)] and imaging was conducted at 20 fps with 2000 lpf. Imaging was conducted for 90 sec, 15 sec prior to the start of rf energy delivery, 60 sec during energy delivery, and 15 sec after the conclusion of energy delivery [Fig. 2(b)]. RFA lesions were created with a temperature-controlled (80 °C) protocol with a maximum delivered power of 50 W using the Maestro 3000 generator and 8-Fr, 5-mm tip catheter Blazer II (Boston Scientific, Natick, Massachusetts). Staining with 1.0% triphenyltetrazolium chloride in PBS for 30 min at 37 °C was used to validate lesion formation [Fig. 2(g)]. Baseline images show a birefringence-dependent dark band characteristic of healthy, untreated myocardium [Fig. 2(c)]. With the application of rf energy, the band broadens and appears deeper in the tissue [Figs. 2(d)–2(f)]. It is important to note that the rf energy, and the temperature rise during energy delivery, did not affect the image quality nor the mechanical stability of the catheter.

The effect of the presence of blood was evaluated by imaging the ventricular wedge submerged in heparinized swine

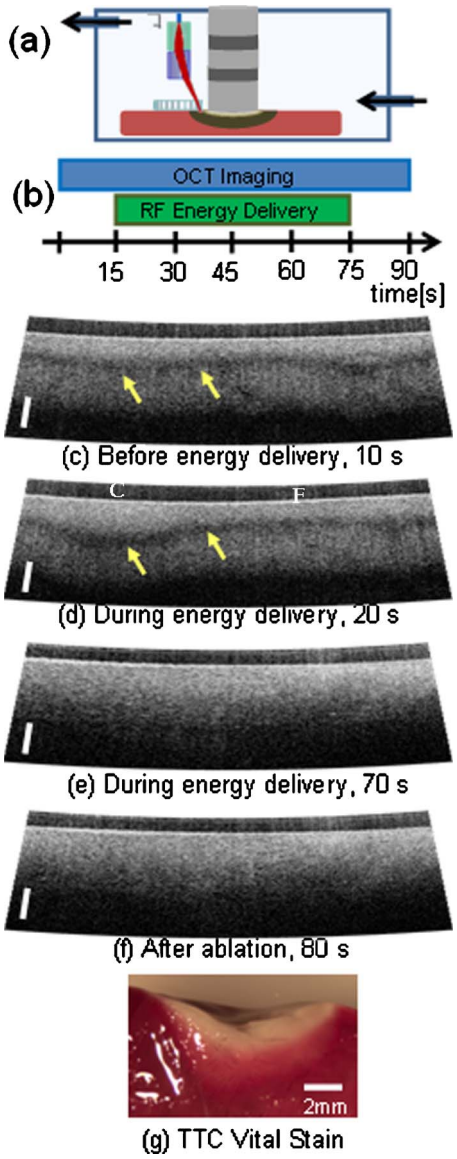

Fig. 2 Visualization of dynamics due to rf energy delivery. (a) Samples placed in custom chamber with superperfusion flow of PBS. Forward-imaging catheter bound side by side to rfa catheter. (b) OCT imaging conducted over 90 sec and 60 sec of rf energy delivery. (c)-(f) OCT images at 10, 20, 70, and 80 sec. Baseline images characterized by birefringence artifact band (arrows). With the application of rf energy, location of birefringence artifact bands lower and then disappear. Scale bar 500 μm. Region closer and further from rfa catheter labeled as C and F, respectively. (g) TTC vital staining, necrotic tissue white and viable tissue red. (Color online only.)

blood. An image of the myocardium was obtained when the catheter was in direct contact with the tissue, displacing the blood (Fig. 3). Blood strongly attenuates light at 1310 nm. When the catheter probe was not in direct contact with the tissue, the imaging depth was significantly reduced [Fig. 3(b)]. An important factors that affect lesion size is the maintenance of tissue-rfa electrode contact. This visual feedback could allow assessment of contact.

3 Discussion and Conclusion

We demonstrate a flexible forward-imaging OCT catheter made without metal that provides circular scanning by proxi-

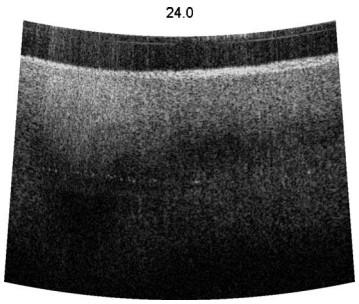

Video 1 Real-time visualization of dynamics due to rf energy delivery. Baseline imaging of 15 sec before the start of 60 sec of RF energy delivery on the Endocardium of the left ventricle (QuickTime 3.9 MB). [URL: http://dx.doi.org/10.1117/1.3459134.1].

mal actuation of the fiber. Using a forward-imaging catheter, we show that OCT can provide real-time direct visualization of rfa therapy, assessing tissue-electrode contact visualizing lesion formation, and can image in the presence of blood. The current design is optimized for the case when the rf catheter has adequate near-perpendicular contact with the tissue surface. For nonoptimal cases, contact angle can potentially be determined by detecting the surface position as a function of rotation angle. This probe design can be miniaturized and integrated into a rfa catheter for future *in vivo* use, and adapted to other applications where a miniature, flexible forward-imaging OCT probe is needed. A direct image by OCT also has the potential to guide the precise application of rf energy, and to identify normal cardiac structures where ablation could be harmful. Importantly, this advance in catheter technology can decrease the procedural time and radiation exposure to the patient and physician.

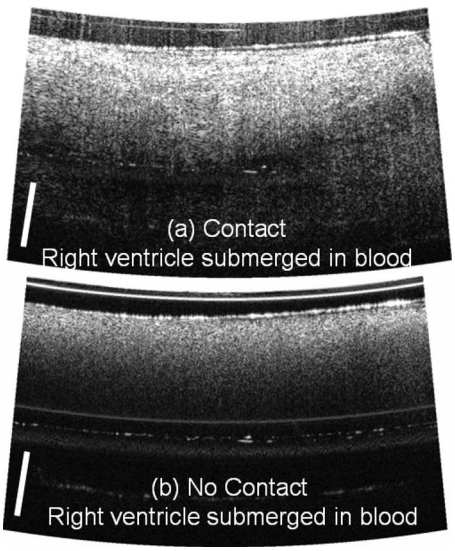

Fig. 3 Assessment of tissue contact in the presence of blood. Sample submerged in heparinized blood. (a) Image obtained when probe was in direct contact with endocardial surface. (b) Imaging depth significantly decreased when probe was not in direct contact with endocardial surface. Scale bar 500 μm.

Acknowledgments

The authors thank Steve Schomish for his technical assistance and Avo Photonics for prototyping the catheter. The project was supported by the Wallace H. Coulter Foundation and by the NIH (F31HL085939, R01HL083048, and RR1246). The content is solely the responsibility of the authors and does not necessarily represent the official views of the National Heart Lung and Blood Institute or the NIH.

References

1. W. Rosamond, K. Flegal, K. Furie, A. Go, K. Greenlund, N. Haase, S. M. Hailpern, M. Ho, V. Howard, B. Kissela, S. Kittner, D. Lloyd-Jones, M. McDermott, J. Meigs, C. Moy, G. Nicho, C. O'Donnell, V. Roger, P. Sorlie, J. Steinberger, T. Thom, M. Wilson, and Y. Hong, "Heart disease and stroke statistics 2008 update: a report from the American Heart Association Statistics Committee and Stroke Statistics Subcommittee," *Circulation* **117**, e25–e146 (2008).
2. J. F. Ren and F. E. Marchinski, "Utility of intracardiac echocardiography in left heart ablation for tachyarrhythmias," *Echocardiogr.* **24**, 533–540 (2007).
3. D. Huang, E. A. Swanson, C. P. Lin, J. S. Schuman, W. G. Stinson, W. Chang, M. R. Hee, T. Flotte, K. Gregor, C. A. Puliafito, and J. G. Fujimoto, "Optical coherence tomography," *Science* **254**, 1178–1181 (1991).
4. C. P. Fleming, K. J. Quan, H. Wang, G. Amit, and A. M. Rollins, "In vitro characterization of cardiac radiofrequency ablation lesions using optical coherence tomography," *Opt. Express* **18**, 3079–3092 (2010).
5. W. Hucker, C. Ripplinger, C. P. Fleming, V. Fedorov, A. M. Rollins, and I. R. Efimov, "Bimodal biophotonic imaging of the structure-function relationship in cardiac tissue," *J. Biomed. Opt.* **13**, 054012 (2008).
6. C. P. Fleming, C. Ripplinger, B. Webb, I. R. Efimov, and A. M. Rollins, "Quantification of cardiac fiber orientation using optical coherence tomography," *J. Biomed. Opt.* **13**, 030505 (2008).
7. D. C. Adler, C. Zhou, T. H. Tsai, J. Schmitt, Q. Huang, H. Mashimo, and J. G. Fujimoto, "Three-dimensional endomicroscopy of the human colon using optical coherence tomography," *Opt. Express* **17**, 784 (2009).
8. G. J. Tearney, S. Waxman, M. Shishkov, B. J. Vakoc, M. J. Suter, M. I. Freilich, A. E. Desjardins, W. Y. Oh, L. A. Bartlett, M. Rosenberg, and B. E. Bouma, "Three-dimensional coronary artery microscopy by intracoronary optical frequency domain imaging," *JACC: Cardiovasc. Imag.* **1**, 752 (2008).
9. N. R. Munce, A. Mariampillai, B. A. Standish, M. Pop, K. J. Anderson, G. Y. Liu, T. Luk, B. K. Courtney, G. A. Wright, I. A. Vitkin, and V. X. D. Yang, "Electrostatic forward-viewing scanning probe for doppler optical coherence tomography using a dissipative polymer catheter," *Opt. Lett.* **33**, 657–659 (2008).
10. J. Wu, M. Conry, C. Gu, F. Wang, Z. Yaqoob, and C. Yang, "Paired-angle-rotation scanning optical coherence tomography forward-imaging probe," *Opt. Lett.* **31**, 1265–1267 (2006).
11. X. Liu, M. J. Cobb, and Y. Chen, "Rapid-scanning forward-imaging miniature endoscope for real-time optical coherence tomography," *Opt. Lett.* **29**, 1763–1765 (2004).
12. J. Xi, L. Huo, Y. Wu, M. J. Cobb, J. H. Hwang, and X. Li, "High-resolution OCT balloon imaging catheter with astigmatism correction," *Opt. Lett.* **34**, 1943 (2009).
13. P. R. Herz, Y. Chen, A. D. Aguirre, K. Schneider, P. Hsiung, and J. G. Fujimoto, "Micromotor endoscope catheter for in vivo, ultrahigh resolution optical coherence tomography," *Opt. Lett.* **29**, 2261–2263 (2004).
14. K. H. Kim, B. H. Park, G. N. Maguluri, T. W. Lee, F. J. Rogomentich, M. G. Bancu, B. E. Bouma, J. F. de Boer, and J. J. Bernstein, "Two-axis magnetically-driven MEMS scanning catheter for endoscopic high-speed optical coherence tomography," *Opt. Express* **15**, 18130–18140 (2007).
15. Z. Hu and A. Rollins, "Fourier domain optical coherence tomography with a linear-in-wavenumber spectrometer," *Opt. Lett.* **32**, 3524–3527 (2007).